HIGHLIGTS

Beachrock as sea level changes indicator

Paleosol on a beachrock can be a coastal progradation indicator

LMC micritic cementation in a beachrock was interpreted as an abundant meteoric groundwater

Upper Quaternary coastal palaenvironments and palaeosea-levels in Las Canteras beach, Gran Canaria (Canary Islands, Spain)

Inmaculada Menéndez[1*], Catalina Herrera-Holguín[1], José Mangas[1]

[1]Instituto Oceanografía y Cambio Global, IOCAG, Edificio Ciencias Básicas, Campus Tafira, Universidad de Las Palmas de Gran Canaria 35017, Islas Canarias, España.

**Corresponding author: inmaculada.menendez@ulpgc.es / +34 928 45 29 22 (fax)*

Upper Quaternary coastal palaenvironments and palaeosea-levels in Las Canteras beach, Gran Canaria (Canary Islands, Spain)

Inmaculada Menéndez[1*], Catalina Herrera-Holguín[1], José Mangas[1]

[1]*Instituto Oceanografía y Cambio Global, IOCAG, Edificio Ciencias Básicas, Campus Tafira, Universidad de Las Palmas de Gran Canaria 35017, Islas Canarias, España*.

**Corresponding author: inmaculada.menendez@ulpgc.es / +34 928 45 29 22 (fax)*

ABSTRACT

Las Canteras beach outcrops correspond to vestiges of palaeoenvironments that represent changes in the sea level and/or climate conditions. Under broad sedimentological, mineralogical, geochemical and dating studies, different palaeoenvironmental facies has been characterised. (1) The lower level has been defined as a beachrock, formed by decametric calcarenitic layers, dipping 8-5° seawards, and composed mainly of sand grains and two generations of isopaque low magnesium calcite (LMC) cement, in a context of a rising sea level, but a coastal progradation, during the lower Holocene Interglacial stage (>6.6 ka). (2) Throughout middle Holocene (about 6.6 ka, ^{14}C dating), coastal progradation phase and/or lower sea level might lead land emersion and soil development, with the presence of abundant terrestrial gastropods. (3) Overhead, founded only in the central arc of the beach, aeoleanites facies from cemented coastal dunes were identified; it was formed by calcarenite levels, dipping 20° landward, cemented by phreatic LMC and vadose aragonite during the upper Holocene (<6.6 ka). This aeolian deposit might represents the highest coast progradation or, the end of low-

stand sea level, whereas its cementation could be interpreted as the beginning of the sea level rise, towards the present highstand sea level situation.

Keywords: coastal palaeoenvironments; palaeosea-levels; coastal progradation; beachrock; palaeosol, aeoleanites; Las Canteras beach; Gran Canaria Island

1. Introduction

The study of coastal palaeoenvironments has been a useful tool to survey local response to global changes (Casalbore et al., 2017; Yao et al., 2017; Jiang et al., 2019). The evolution of such environments change within spatial and temporal scales, being affected by from tidal shifts to eustatic-tectonic processes, climatic influences, moreover, the increasing pressure due to human occupation. Accordingly, coastal environments have been studied worldwide, dealing with reconstructing past environments, including integrated studies, linking diverse geological and biotic records (i.e. Dickinson, 2001; Murray-Wallace, 2002; de Carvalho et al., 2006). Beachrocks are carbonate-cemented on any type of littoral sediments and climate that have been widely used as proxies in Quaternary palaeosea-levels (i.e., Vousdoukas et al., 2007; Desruelles et al., 2009; Mauz et al., 2015; Falkenroth et al., 2019). However, superficial beachrock on coastlines have been rarely dated because of the absence of fossils, the small carbonated crystals and the chronostratigraphic differences in the beachrock layers (Friedman, 2004).

The texture and composition of carbonate cements reflect the cementation environmental conditions (phreatic-marine-vadose). Beachrock cements are typically high-Mg calcite or aragonite, formed in the mixing zone of the intertidal beaches (i.e., Kneale and Viles, 2005;

Vousdoukas et al., 2007; Haredy et al., 2019). Changes in exposure, temperature, salinity, CO_2 degasification and algae activity and overall microorganisms control (McCutcheon et al., 2017) favour its cementation. Beach progradation or slight sea-level fall changes the cementation to vadose and edaphic conditions, producing the dissolution of high-Mg calcite and aragonite and subsequently diagenetic precipitation of LMC (Beier 1985). LMC (meteoric) beachrocks are less common than HMC, but worldwide examples can be found, i.e. Bahamas (Strasser and Davaud 1986), Florida (Spurgeon et al. 2003), Ireland (Cooper et al., 2017), South Africa (Wiles et al., 2018).

Diagenesis involves dissolution, precipitation and recrystallization processes, depleting the cement in Mg, Sr but enriching it with Fe and Mn (Tucker and Wright, 1990). Coastal dunefield can be constructed off the backshore. Phreatic-marine oscillation processes can subsequently cement it, forming aeoleanites (Frébourg et al., 2008).

Along the Canary Islands, HMC beachrocks there have been identified in La Palma (Calvet et al., 2003) and Lanzarote (Mangas et al., 2008) and Fuerteventura (Meco et al., 2018). Coastal palaenvironments and their sedimentary formations such as beachrock, palaeosol and aeoleanites, have been risen due to geological and climatic processes and related to environmental changes (Hernández-Calvento et al., 2002; Hernández-Calvento and Mangas, 2004; Meco et al., 2002, 2011, 2018; Ortiz et al., 2006).

The aim of this research is an integrated study (geochemical, mineralogical, petrographic, geochronological, edaphic and stratigraphic) of the different outcroppings of Las Canteras beach, to provide new proxies in the reconstruction of coastal palaeoenvironments and palaeoshorelines.

2. Regional setting

The Canary Islands is an archipelago located 100–700 km off Western Sahara, on the oceanic crust of Jurassic age (165–176 Ma; Schmincke and Sumita, 2010). Its formation is interpreted as a hotspot volcanism (Schmincke and Freundt, 1990; Walker, 1990; Carracedo et al., 1998). Submarine magmatism took place on the Jurassic oceanic crust, starting with the first submarine lava flows 34 Ma ago, in Fuerteventura island (Schmincke and Freundt, 1990; Carracedo et al., 2002; Schmincke and Sumita, 2010).

In Gran Canaria, the submarine volcanism conform about 97% in volume of the whole volcanic and sedimentary materials of the island (Menéndez et al., 2008). The remaining 3% of the island volume are the subaerial materials, which gather in three magmatic cycles. The first one is associated to Tejeda Caldera and comprises the shield stage, with emission about 1000 km^3 of ultramafic and mafic materials, during Miocene (14.5 - 14.1 Ma), evolving to the alkaline declining stage of intermediate and felsic deposits during 14.1 to 7.3 Ma, emitting, again, about 1000 km^3 of volume material. There was a volcanic inactivity period between 7.3 - 5.3 Ma. The second one is associated with the Roque Nublo stratovolcano, producing a 210 km^3 from ultramafic and mafic materials to felsic, during 5.3 - 2.8 Ma. The third cycle, Post Roque Nublo magmatic cycle, started 3.7 Ma ago, generating ultramafic, mafic and intermediate fissural volcanism and then individual volcanism, occurring the last eruption on 1970 ±70 B.P. (Pico Bandama; Rodríguez-González et al., 2009). Two and third magmatic cycles were defined as rejuvenation stages. During all the cycles, the external geological processes (alluvial, fluvial, coastal and weathering) had been generating sedimentary deposits, such us fan deltas, coastal dunefields and beaches, integrated some of them in Las Palmas Detritic Formation (Fuster et al., 1968; Balcells et al., 1990; Schmincke and Sumita, 1998, 2010; Carracedo et al., 2002; Schneider et al., 2004).

The volcanic bedrocks and outcropping in the area of Las Canteras beach, are associated with alkaline declining (phonolite lava and ignimbrites) and rejuvenation stages (basaltic lava flows and pyroclastic deposits). Sedimentary deposits of the LPDF (sandstones and conglomerates) were also identified on the north arc of Las Canteras beach (Pérez-Torrado and Mangas, 1992; Pérez-Torrado et al., 2000). Las Canteras sandy beach, is an urban space with significant social, touristic, and environmental value (Santana-Cordero et al., 2017). Outcropping in the central part of Las Canteras beach there are several calcarenitic formations (beachrock), acting the external part as an offshore barrier (locally known as La Barra) causing a reduction on wave energy on the inner beach, (Alonso, 1993, 1994, 2005; Alonso and Vilas, 1994; Martínez-Martínez et al., 1990; Pérez-Torrado and Alonso, 1992; Pérez-Torrado et al., 2000). La Barra was dated as Jandian, 110 ka (Balcells et al., 1990; Pérez-Torrado and Mangas, 1992). It was interpreted as an intertidal cementation during Riss Glaciation (>130 ka; Alonso, 1993; Alonso and Vilas, 1996). La Barra has experienced about 29% mining reduction (Ferrer-Valero et al., 2017). The inner beachrock part appears as isolated outcrops in the foreshore of the Las Canteras beach. It consisting of a set of decimetric parallel layers, dipping 8-15° seawards (Pérez-Torrado et al., 2000). In this work, we only focus on this inner beachrock of the central arc of Las Canteras beach.

On the upper part of the beachrock, a pinkish silty-clayey formation with terrestrial gastropods and vegetal bioturbation has been reported (Pérez-Torrado and Mangas, 1992; Pérez-Torrado et al., 2000; Alonso, 1993). It was twofold interpretation, as a palaeosol

(Alonso, 1993), and as a lagoon (Pérez-Torrado et al., 2000). Finally, another different deposit outcropping at the southern and landward part of the Las Canteras central arc. It was described as eolianites, dipping about 20° landward, and formed in backshore conditions (Pérez-Torrado et al., 2000), accordingly to Alonso (1993) it could be formed during the Flandrian period (10 ka).

3. Material and Methods

3.1. Site

Las Canteras is an approximately 3 km long sandy beach, located on the northeastern coast of Gran Canaria, within the Confital Bay, on the east side of Guanarteme isthmus, which connects the city of Las Palmas de Gran Canaria with La Isleta headland (Fig. 1). Indicating the position of a palaeocoastline appears La Barra, approximately 1600 m long and 50-100 m width, whose elevation is similar to the mean sea level (MSL), therefore during low tide it generates a sheltered area where the wave action is reduced (Pérez-Torrado and Mangas, 1992; Alonso, 2005). This barrier, parallel to the coast, separated about 200 to 250 m from the shoreline, have significant impact in this specific beach sedimentary dynamics (Martínez-Martínez et al., 1990; Alonso, 1993, 1994, 2005; Alonso and Vilas, 1994), formerly an extended coastal dunefield completely disappeared through resource exploitation and urbanisation (Santana-Cordero et al., 2017).

There are three different sectors on this semi-enclosed beach (Fig. 1): the southern arc, where there are substantial losses of sediment erosion during storms (Alonso, 1993; Alonso and Vilas, 1994). The central arc, located about 750 m long, is partially sheltered by La

Barra, and the focus of the study. Sedimentary budget variations in this arc are fewer than in the south and north arcs (Casanova, 2015). Finally, the northern arc, sheltered excepting the north end, present sand accumulation from southern arc erosion (Alonso, 1993; Alonso and Vilas, 1994; Casanova, 2015).

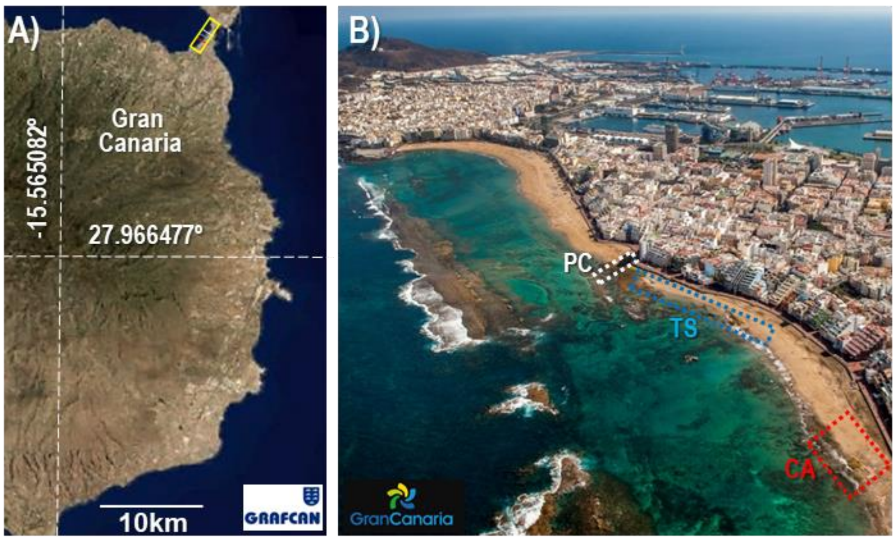

Figure 1. (A) Location of Las Canteras beach (yellow rectangle) on the northeast coast of Gran Canaria Island, (B) Aerial photo of Las Canteras beach in the city of Las Palmas de Gran Canaria, showing Playa Chica (PC) section within the white rectangle, Transition Section (TS) within the blue rectangle, and Colombia Area (CA) section within the red rectangle. Modified from A) Grafcan (https://www.grafcan.es/), and B) the touristic blog of the Cabildo of Gran Canaria (http://www.grancanaria.com/blog/es/article/gran-canaria-segun-carla-suarez/).

3.2. Sampling procedure

Three sections were chosen for sampling: Playa Chica (PC), a transition section (TS) and Colombia area (CA; Fig.1B). The PC section is a semi-enclosed beach environment, whereas the CA is at the southward end of the central arc and more affected to wave action. To maximise the intertidal exposure, the campaign was synchronised with a spring low tide, on September 17th 2017, 8:00 h. Geographical coordinates were taken at each sample point (Table 1). The collected amount of each sampled rock was 0.5-1 kg, and 0.1 to 0.5 kg for sediment. Current beach sands information and additional 5 samples were provided by Dr. Ignacio Alonso courtesy.

Table 1. Identification, coordinates, location and geological material of the Samples from the palaeoenvironmental study of Las Canteras beach. A6-10 samples information from Alonso, 1993.

Sample	Longitude (W)	Latitude (E)	Section	Description
PAC1	15°26'11"	28°8'23"	Playa Chica (PC)	Beachrock
PAC2	15°26'11"	28°8'22"	"	"
PAC3	15°26'10"	28°8'22"	"	"
PAC4	15°26'10"	28°8'22"	"	"
PAC5	15°26'10"	28°8'22"	"	Palaeosol
PAC6	15°26'10"	28°8'22"	"	"
PAC7	15°26'10"	28°8'22"	"	"
PAC8	15°26'10"	28°8'22"	"	Gastropods

PAC9	15°26'10"	28°8'22"	“	Palaeosol
PAC10	15°26'10"	28°8'22"	“	“
PAC11	15°26'10"	28°8'22"	“	“
PAC11B	15°26'10"	28°8'22"	“	“
A10	15°26'10"	28°8'22"		Current sands
PAC13	15°26'13"	28°8'16"	Transition S. (TS)	Beachrock
PAC12	15°26'11"	28°8'20'	“	Palaeosol
PAC14	15°26'13"	28°8'14"	“	“
A9	15°26'13"	28°8'16"	“	Current sands
A8	15°26'13"	28°8'16"	“	“
PAC15	15°26'21"	28°8'10"	Colombia Area (CA)	Beachrock
PAC16	15°26'21"	28°8'9"	“	Palaeosol
PAC17	15°26'21"	28°8'9"	“	“
PAC18	15°26'21"	28°8'9"	“	“
PAC19	15°26'21"	28°8'9"	“	“
PAC20	15°26'21"	28°8'9"	“	Aeoleanites
A7	15°26'21"	28°8'9"	“	Current sands
A6	15°26'21"	28°8'9"	“	“

3.2. Grain size distribution and carbonate content

Grain size analyses was made on three uncemented palaelosols samples (PAC11, PAC11b and PAC17, Table 1). In order to reduce the aggregates, a sodium hexametaphosphate was used. It was prepared by mixing 5g ($Na_6O_{18}P_6$) in 1000 ml of distilled water (Sperazza et al., 2004). The dispersion was conducted by adding the solution in a 2:1 stirring during 48 h. After 8h of decantation the clays grain size in suspension was removed and dried. The rest sediment material (silt and sand) was dried and mechanically fractionated thought 2 and 0.045 mm seizes. The GradiStat V8® free software (Blott and Pye, 2001) was used to statistical determination.

The calcium carbonate content was determined by the volumetric method of the Bernard calcimeter, by the hydrochloric acid leaching and CO_2 measurement technique (Hulseman 1966).

3.3. Petrography

In order to identify their components and its relative abundance, 19 thin sections were prepared besides 5 previous of sand samples from Alonso (1993). Thin sections were made in the General Geology Services of the Universidad de Salamanca. The petrographic study of the thin sections were made under a geologic microscope (Ortoplan-Leitz) with a pointer counter stage (PETROG). The subcategories observed were: (i) bioclastic grains: seaweed mesh, foraminifera, mollusk, echinoderm and other bioclasts), (ii) lithoclastic grains: mafic rock fragment, felsic rock fragment, intraclast, olivine, pyroxene, opaque, feldspar, amphybole and others lithoclasts, (iii) carbonate cements: sparitic and micritic, and (iv) soil features: palaeosol matrix and cutans. Finally, the rock porosity was quantified as the void surface (holes).

3.4. XRD, EMPA and SEM-EDX analysis

Uncemented samples of the palaeosol (PAC 11, PAC11b and PAC17) were sent to the Geology Laboratory of La Laguna University for mineral phase identification by X-ray diffraction (XRD). Samples of the selected profiles were crushed in an agate mortar, obtaining a particle size below 40 mm. The experimental profiles were performed using a PANalytical Empyrean powder diffractometer equipped with a PIXcel1D Medipix 3 detector at the XRD Integrated Service (SIDIX) of the *Servicio General de Apoyo a la Investigación* (SEGAI) of La Laguna University (ULL). The diffractometer equipment was used with incident Cu Kα12 radiation at 45 kV and 40 mA, and it was equipped with a RTMS detector (PIXcel1D) with an amplitude of 3.3473° 2θ. The patterns were obtained by scanning random powders from 5° to 80° (2θ). Data sets were obtained by a scan time of 57s at a step size of 0.0263° (2q) and a 1/16° divergence slit. Mineral identification and semi-quantitative results were facilitated using the Highscore Plus version 4.5 from PANalytical B.V search-match software with PDF+ crystallographic database. When the occurrence of quartz was detected in the sample it was used an internal standard to correct diffraction patterns for instrumental shifts in 2q position. Quantitative mineral phase analyses were obtained by full refinement profile using the software TOPAS V4.2.

The rocky samples were mineralogy and geochemical analysed by Scanning electron Microscope equipped with an energy-dispersive spectrometer (SEM-EDX) and Electron Microprobe Analysis (EMPA) at the Scientific and Technological Centre of the University of Barcelona (CCITUB). Experimental conditions detailed in (Menéndez et al., 2019). The $MgCO_3$ and Sr contents of the different types of cement were also determined.

3.5. Carbon dating

In order to calculate the age of palaeosol, some gastropods (*Helix* sp.) were collected in the upper part of PC Section and sending for ^{14}C radiocarbon dating to Beta Analytic Radiocarbon Dating Laboratory (Florida, USA). By international convention, the modern reference standard was 95% the ^{14}C activity of the National Institute of Standards and Technology (NIST) Oxalic Acid (SRM 4990C) and calculated using the Libby ^{14}C half-life of 5568 years. Calibrations were calculated using the 2009 calibration database (Talma and Voguel, 1993) within the mathematics used for calibration scenario by Stuiver and Braziunas (1993). Dates were reported as RCYBP (radiocarbon years before present; present: AD 1950).

3.6. Stratigraphy

Facies identification was made and stratigraphic columns and correlation were built to obtain a space and time relationship of the materials in each section, and a further interpretation and reconstruction of their palaeoenvironmental history. The field information and the mentioned analyses were incorporated for integration purposes.

4. Results

4.1. Facies definition

After examination the samples analysis, along with the field data observations, the identified facies, from bottom to top, were (Fig. 2): (1) Beachrock, on which (2) Palaeosol was developed, covered only in CA (3) by Aeoleanites; surrounding all the outcrops are the (4) Current sands. The beachrock can be observed in the three sections. Mainly consists of 5 to 20 cm bands of intertidal calcarenites with dips ranging from 5º (CA) to 15º (PC). Palaeolosol can be subdivided into two subfacies: A stratum formed by tabular calcareous bands sub horizontal, which represent the weathering horizon (C-H) and a discontinuous bed of silty sands, which represent the accumulation horizon (B-H) with abundant terrestrial gastropods (*Helix* sp.) and observable cemented bioturbation (rhizoliths). Aeoleanites are calcarenites with wide-angle (~20º) stratification, dipping towards land, associated to backshore dunes. Current sands are coarse to medium light-coloured sands with good to moderate sorting.

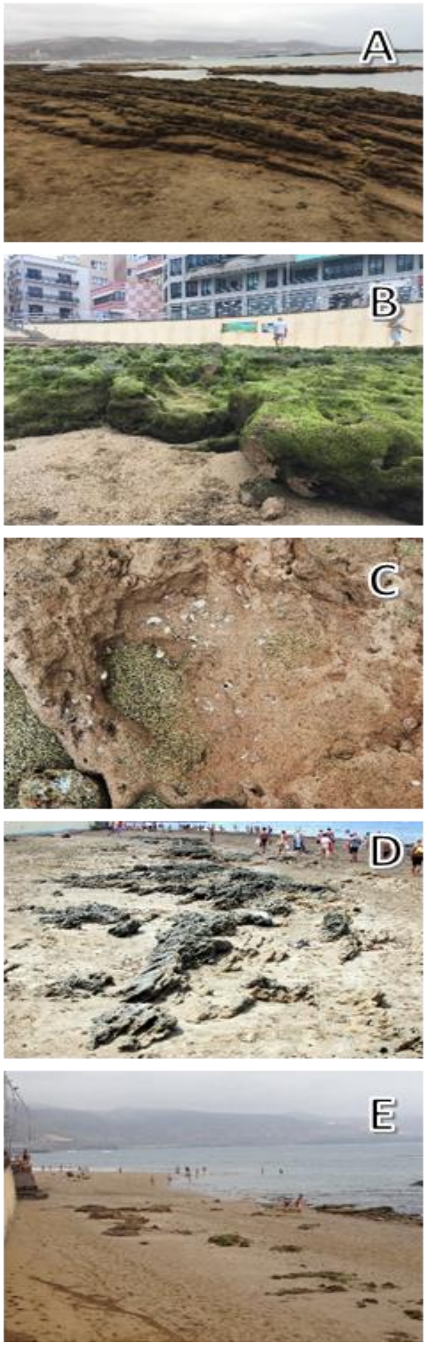

Figure 2. Identified facies in Las Canteras beach: (A) Beachrock in PC; (B-C) Palaeosol in PC; (D) Aeoleanites in CA; (E) Current sands in the central arc; current sands information from Alonso (1993).

The vertical distribution of the facies in each section is equivalent, appearing the outcropping beachrock located between the foreshore and shoreface, the palaeosol in the intertidal and the aeoleanites in the backshore and foreshore (Fig. 3). On PC, the tabular sections of the palaeosol are thicker and greater is the volume of buried terrestrial gastropods and bioturbation than in TS and CA. TS presents more fractures than the rest and in CA aeoleanites facies outcrops grow or reduced their extension more frequently regarding erosion-sedimentation dynamic of the Current sand facies.

Figure 3. Sedimentary outcrops of the three different sections along Las Canteras beach (see Fig 1B). Dotted lines: Beachrock limits (blue), Palaeosol limits (magenta) and Aeoleanites limits (yellow). A) PC S-N view. B) PC E-W view. C) TS S-N view. D) TS E-W view. E) CA N-S view. F) CA E-W view.

4.2. Grain size distribution and carbonate content

The analysis of uncemented samples of the palaeosol (PAC11, PAC11b and PAC17) correspond to clayey to muddy sands (Table 2; Figs. 4-5). The samples were not unimodal thus the sorting, skewness and kurtosis statistics are therefore unreliable. The 1st mode is coarser, and equal, in PAC11 and PAC11B (coarse sand) than in PAC17 (very fine sand). However, 2nd mode is equal value in for PAC11B and PAC17 (medium sand), also shearing mode 3rd and mode 1st value (medium sand).

Table 2. Main textural results from the grain size distribution analyses of the three uncemented samples of Las Canteras beach.

	Playa Chica		Colombia Area
	PAC11	PAC11B	PAC17
Sample type	bimodal, very poorly ported	polymodal, extremely poorly ported	trimodal, extremely poorly ported
Textural group	muddy sand	muddy sand	muddy sand
Sediment name	muddy-coarse Sand	clayey-medium sand	muddy-medium sand
Geometric mean grain size (µm)	479	340	255
1st mode (µm)	605	605	153

2nd mode (µm)	108	303	303
3rd mode (µm)	-	153	54

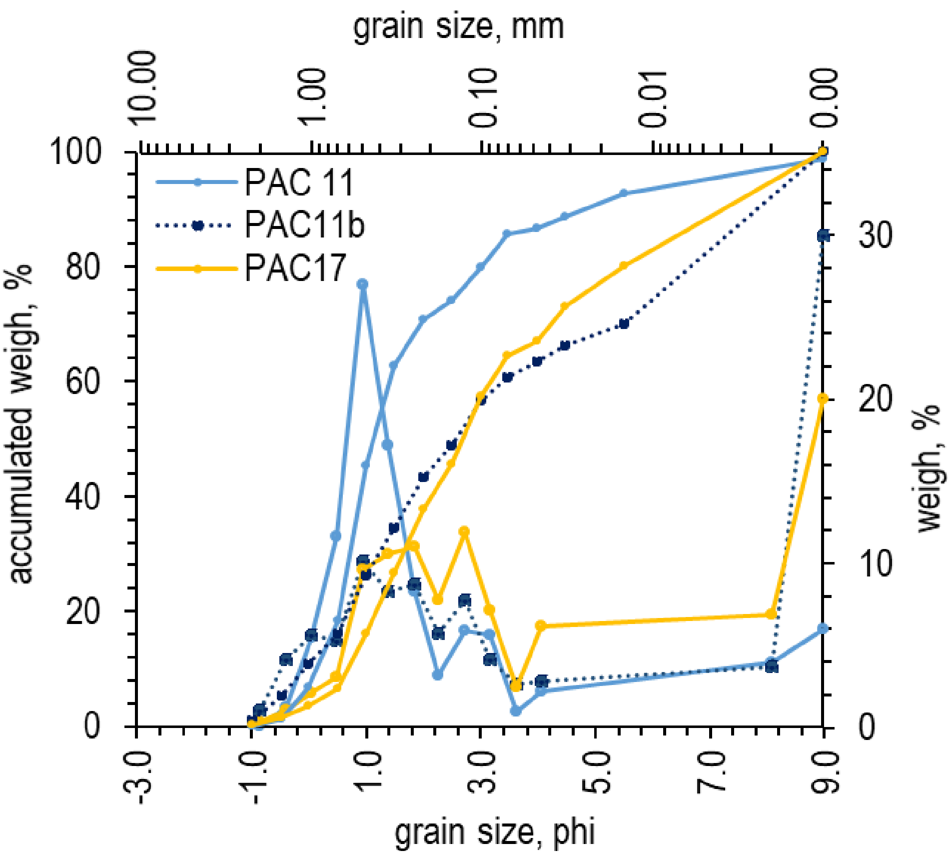

Figure 4. (A) Grain size distribution of uncemented palaeosol samples from Las Canteras beach. (B) Cumulative grain size distribution curves.

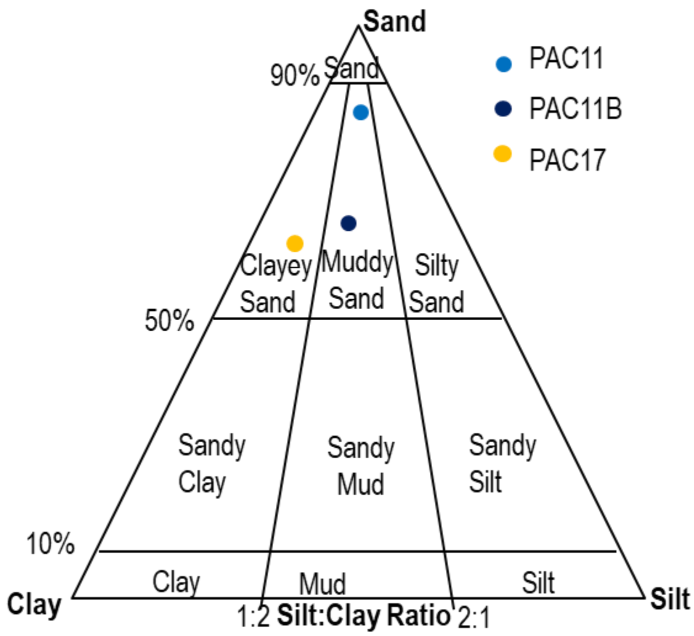

Figure 5. Textural classification of the uncemented palaeosol samples from Las Canteras beach.

The inorganic carbon analysis indicated a high content of carbonates in all samples, with mean beachrock values 82%, being the highest in TS (Table 3). Palaeosol mean carbonate content decrease particularly in TS (70%). Aeoleanites carbonate content is similar to beachrock but markedly reduced in the uncemented current sands.

Table 3. Carbonate content, in %, of the facies and sites defined in Las Canteras beach outcrops. Analysis made by Bernard Method.

		Carbonate Content, %		
Facies	Section	mean	sd	n
	PC	80	±6	4
Beachrock	TS	84	±0	2
	CA	84	-	1
	mean	*82*	*±5*	*7*

	PC	71	±8	7
Palaeolosol	TS	59	±12	4
	CA	82	±3	2
	mean	*70*	*±11*	*1.3*
Aeoleanites	CA	82	-	1
Current	PC	49	-	1
Sands	TS	48	±1	2
	CA	53	±1	2
	mean	*50*	*±3*	*5*

4.3.Petrography

In Figs. 6-8, the most relevant petrographic components from thin sections are displayed. Despite the differences between facies, petrographic results show that seaweed meshes and mollusc (30-5% and 9-5%, respectively) constitute mainly the bioclasts. The bioclasts are more abundant in Beachrock facies (50%). Carbonate cements are more abundant in Aeoleanites facies (37%). Sparitic cement is more abundant than micritic (33-5% *vs.* 4-1%). The proportion of lithoclast is similar in all facies (27-23%) except to the uncemented Current sands, whereas is greater (37%). Lithoclast are composed mainly of sedimentary intraclasts and felsic rocks fragments (14-4% and 12-4%, respectively). The intraclasts are mainly carbonates, formed by grains of bioclasts and minor amount of lithic fragments, imbued in the silty matrix of the palaeosol, or in carbonated cement of the eolianite and beachrock. The cement form a ring around the grains but the pore spaces remain empty in the centre most of the time, or infill the intragranular porosity. The mean porosity ranges from 29% in Current sands to 8% in Aeoleanites facies. There is also a porosity reduction in TS and PA Palaeosol facies regarding the Beachrock parent rock, but an increase for CA.

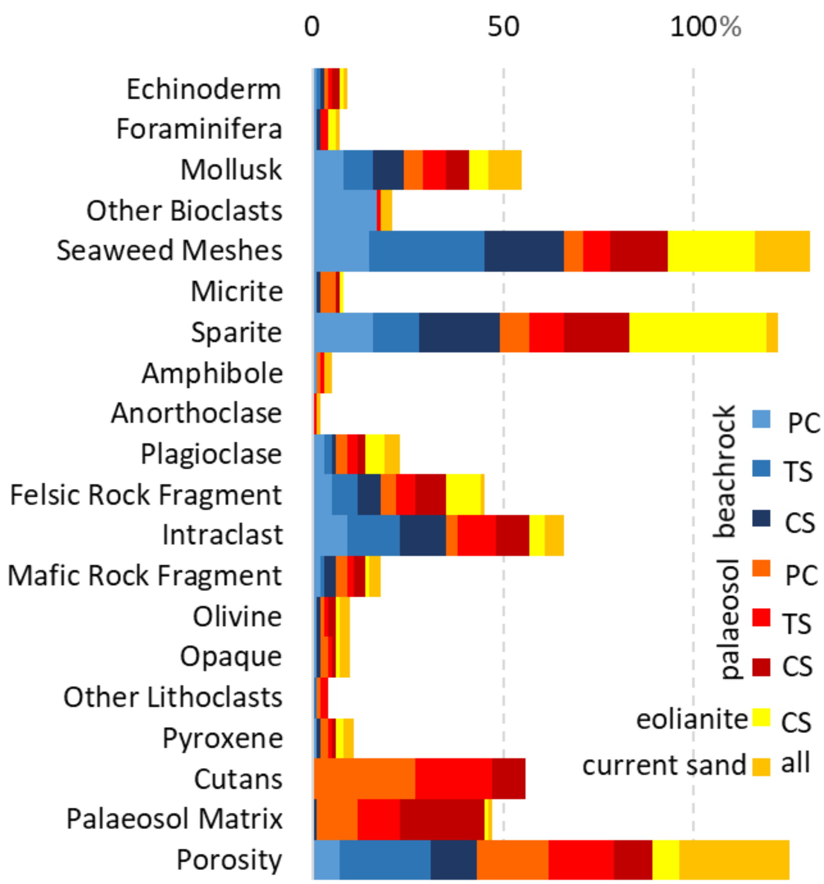

Figure 6. Main observed components (bioclasts, lithoclast, cements, soil features and porosity) under the petrographic microscope, of the thin sections from Las Canteras samples.

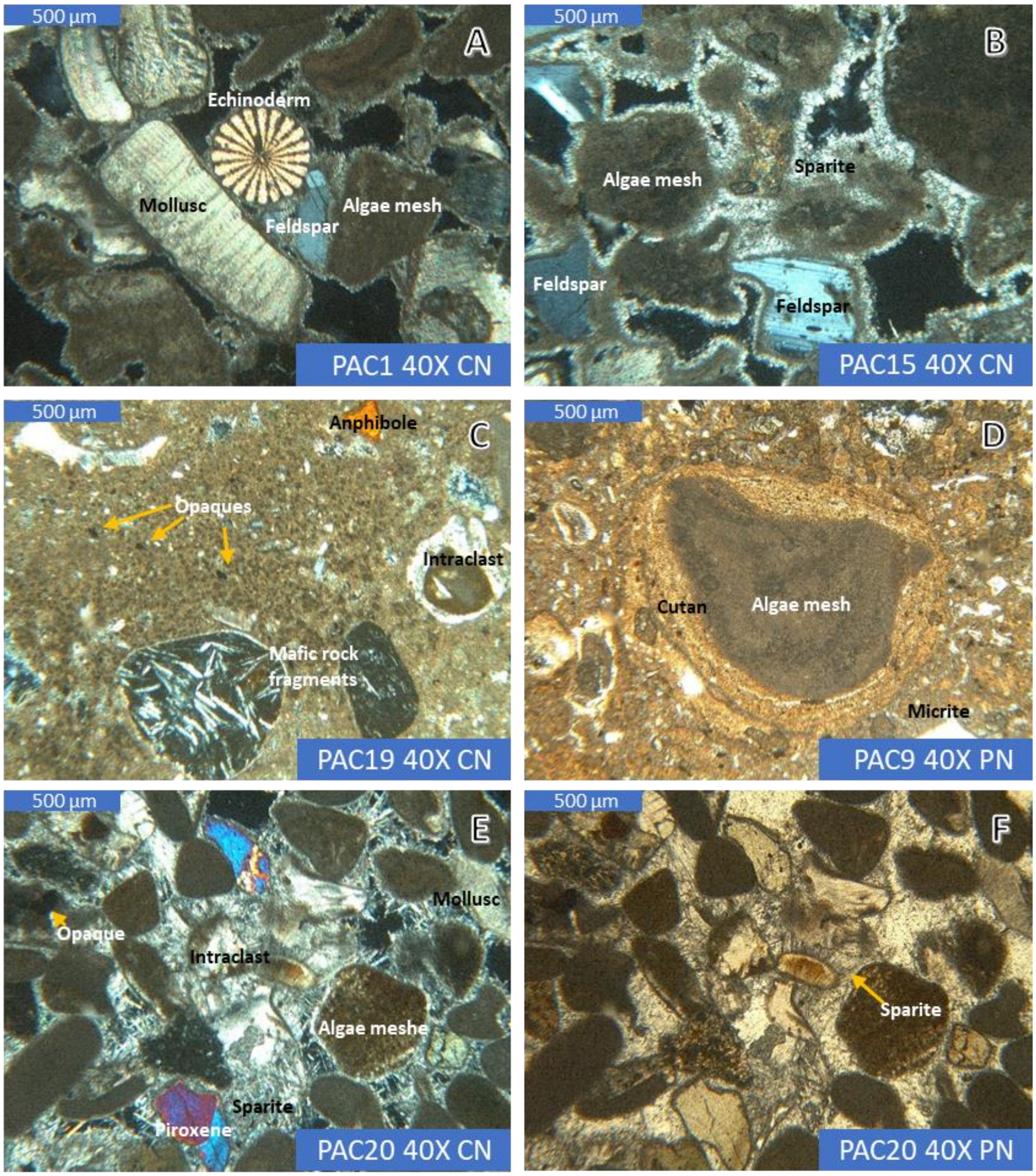

Figure 7. Petrographic microscopy images showing some biogenic and lithogenic components. A and B: sparite as an isopaque calcite cement; C and D: micrite as clay and silt particles with micritic calcite cement; E and F: sparite as isopaque calcite and prismatic aragonite cement. Downright blue labels symbols: sample identification (see Table 1), the magnification (40x) and crossed nicols (CN) parallel nicols (PN).

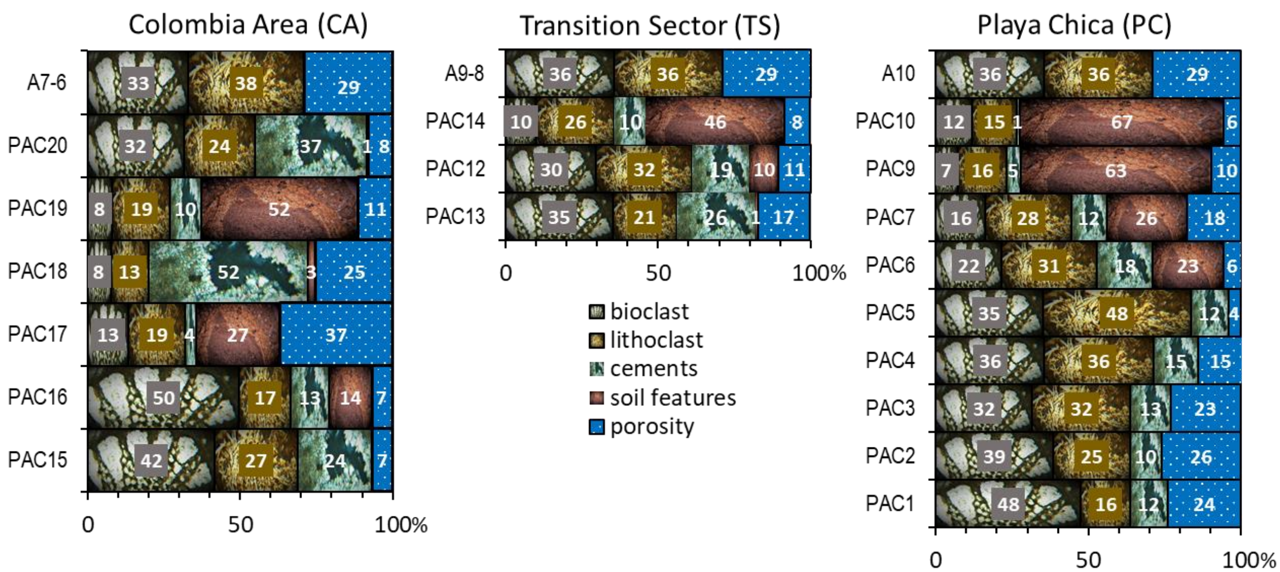

Figure 8. Petrographic features content (in %) from the three sections of Las Canteras beach samples. Current sands information re-elaborated from Alonso (1994). Sample identification in Table 1.

4.4. XR-Diffraction analysis

The XRD semi-quantitative analysis from the uncemented samples identified calcite as the most abundant mineral, with the presence of quartz on all of them and minor amounts of clay minerals (illite, kaolinite and traces of smectite; Table 4; Fig. 9). Minor NaCl peak in PAC11b occurs, due probably to less properly leaching of the sample; it was not computed in the mineralogy quantification.

Table 4. Mineral composition, in percentage, from XR diffraction analysis of uncemented palaeosol samples of Las Canteras beach. *Carbonate content from Bernard Method.

	PC		CA
	PAC11	PAC11B	PAC17
Illite	6	3	3
Kaolinite	0	3	0
Smectite	0	0	3
Quartz	9	61	27
Calcite	85	33	67
Carbonate*	83	21	45

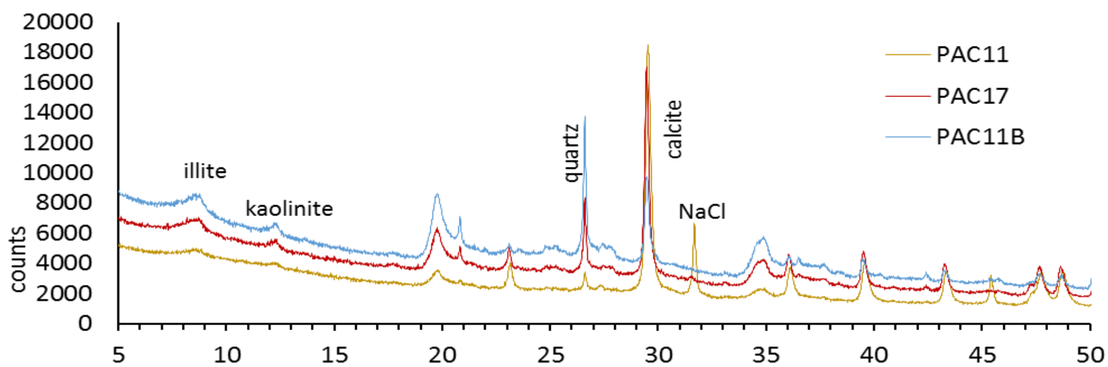

Figure 9. Diffractogram showing the mineralogical composition of the uncemented palaeosol samples of Las Canteras beach.

4.5. SEM and EMPA analysis

The beachrock is a calcarenite with interangular porosity (Fig. 10A-B). The cement is LMC, with Sr and minor amounts of Na, Fe and Mn (Fig. 11A-B). The grain sand are cover with microsparitic and micritic LMC. Aassembling the grains, it was grown a secondary banded isopaque cement (>10µm) composed of sparitic LMC trigonal hexagonal scalenohedral crystals (dogtooth spar calcite, Fig. 10B). It was also observed a random and irregular groups of microcrystalline zeolites, rhombohedral forms (chabazite), seldom and irregular micrite, and salts (chlorides and sulphates).

The palaeosol is a sandstone with a silty matrix that cover most of the grains, forming a banded accumulation of silty silicates and iron oxides/hydroxides (cutans), salts and microcrystalline carbonates (<5µm). Secondary isopaque carbonated cement up to 100µm thickness was grown (Figs. 10C-D, 11C-D). Occasionally, iron banded oxides/hydroxides (>30µm of hematite and goethite) were identified.

The aeoleanites, as the beachrock, is a calcarenite with LMC calcium carbonate isopaque bands in dogtooth spar, but with a secondary cementation of rhombic aragonite (discontinuous and irregular) observed as acicular prismatic crystals, up to 100 µm in length (Figs. 10E-F, 11E-F). Those aragonite crystals are rich in Sr, but Mg is absent (Figs. 11E-F and Table 4). In some grains, the acicular aragonite cluster to zeolites, salts and calcite.

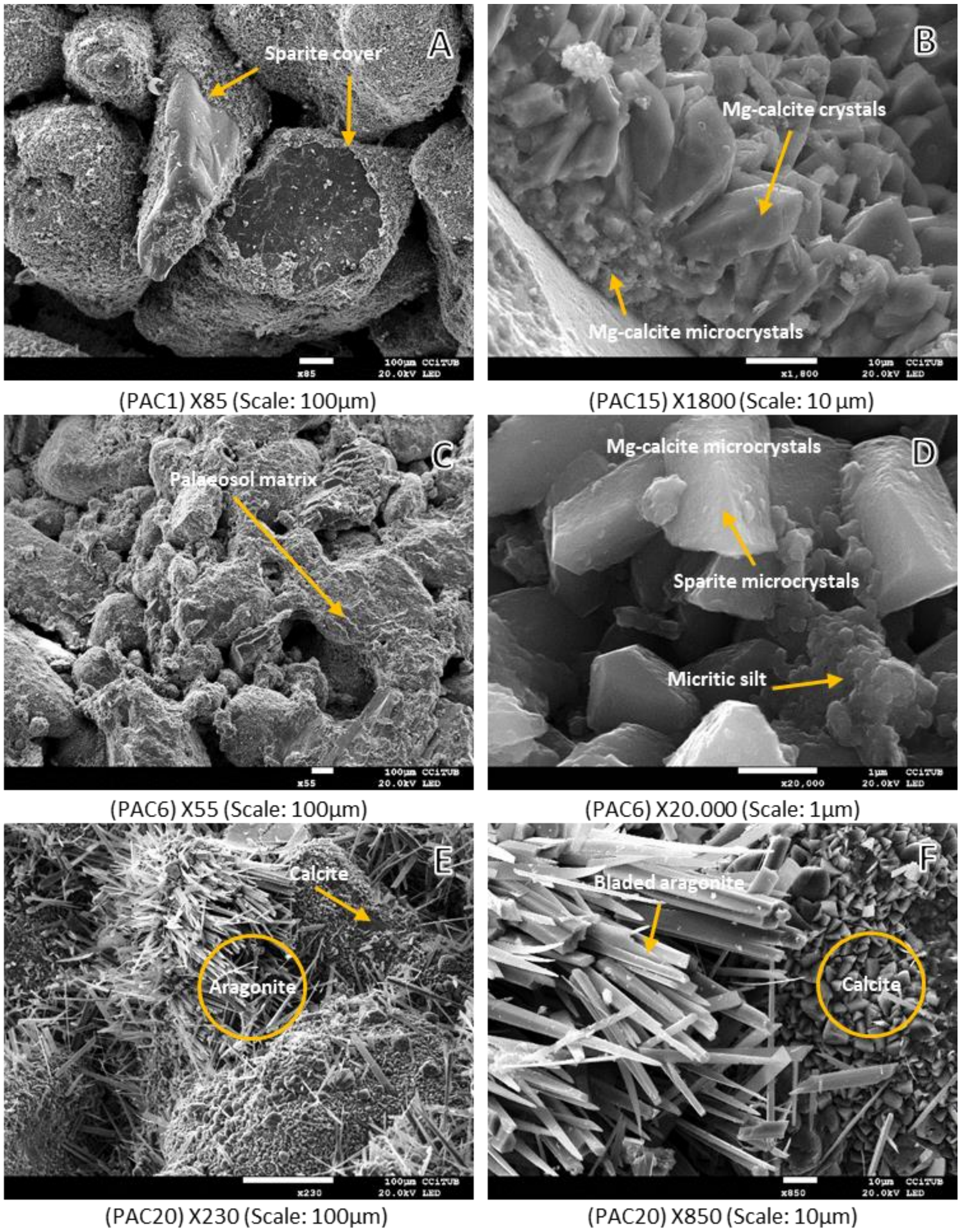

Figure 10. General (left) and detailed (right) views of the SEM images from the Beachrock (A-B), Palaeolosol (C-D) and Aeoleanites facies (E-F) from Las Canteras beach samples. Labels and arrows show the most relevant minerals and features.

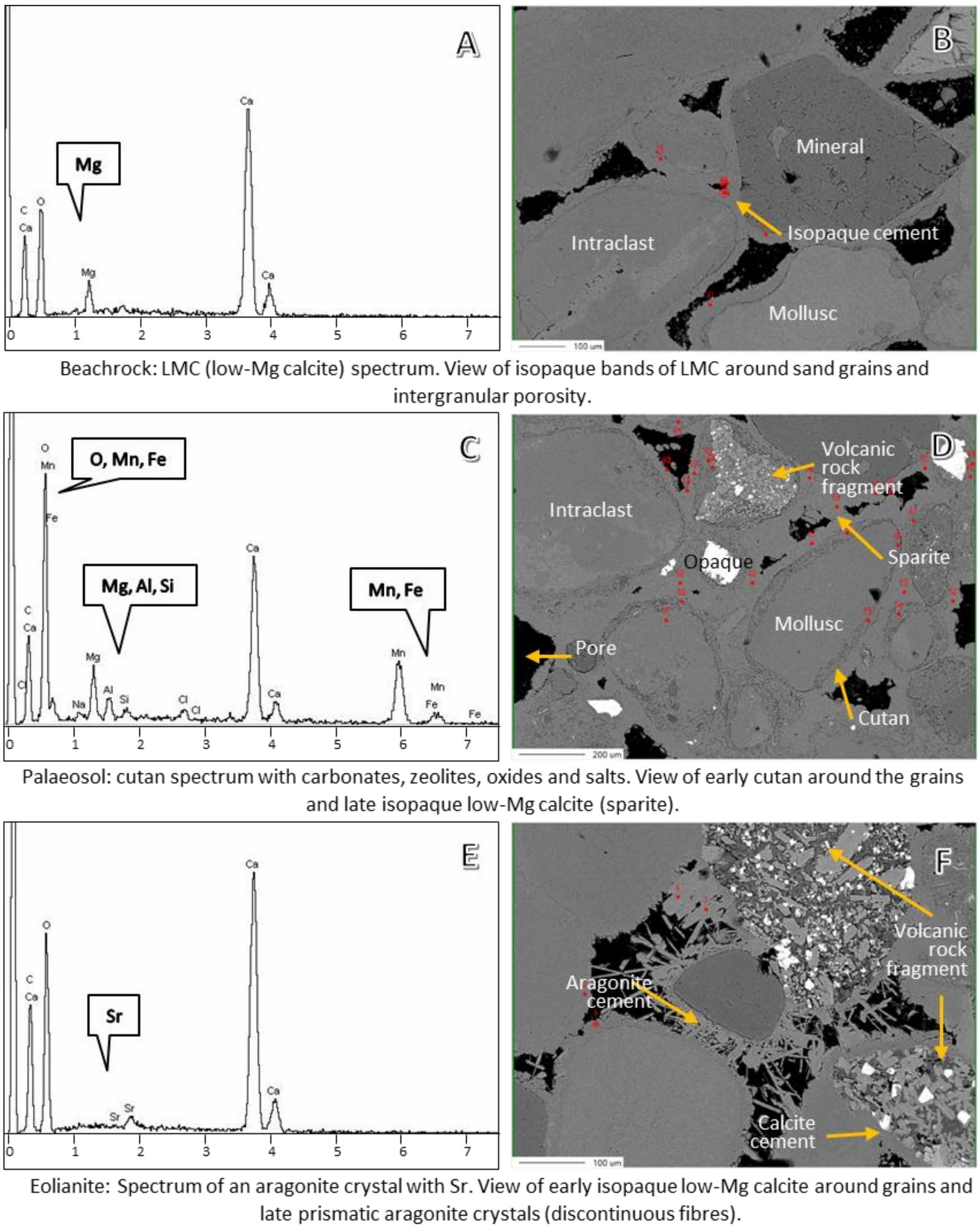

Beachrock: LMC (low-Mg calcite) spectrum. View of isopaque bands of LMC around sand grains and intergranular porosity.

Palaeosol: cutan spectrum with carbonates, zeolites, oxides and salts. View of early cutan around the grains and late isopaque low-Mg calcite (sparite).

Eolianite: Spectrum of an aragonite crystal with Sr. View of early isopaque low-Mg calcite around grains and late prismatic aragonite crystals (discontinuous fibres).

Figure 11. EMPA mineral spectrums showing geochemical relative content of selected points (red markers in right images) from the Beachrock (A-B), Palaeolosol (C-D) and Aeoleanites facies (E-F) from Las Canteras beach samples. Labels and pointers showing relevant elements.

Table 5. Magnesian carbonate, Sr, Na, Fe and Mn molar concentrations of EMPA analysis shown in the carbonates of the Figure 9, for each facies samples.

	CO_3Mg %	Sr ppm	Na ppm	Fe ppm	Mn ppm
LMC-Beachrock	5.2±0.5	1410±509	1150±476	221±144	126±240
LMC-Palaeosol	4.2±0.7	500±231	595±500	339±261	70±147
LMC-Aeoleanites	4.7±1.2	798±806	201±207	285±224	58±90
LMC-Cutans	4.1±1.4	1377±972	972±565	486±597	51±73
Aragonite	0.0±0.0	14129±2635	407±363	106±65	45±105

4.6.Carbon dating on palaeosol facies

The carbon dating was made on gastropods shells collected in the PC palaeosol facies (Fig. 12). These gastropods were abundant, well preserved and randomly integrated in the palaeosol discarding, *a priori*, its later accumulation, and assuming that the soil was their living habitat. The analysis yield a radiocarbon age of 6.60 ± 0.03 ka.

Figure 12. Palaeosol facies in Las Canteras beach (Playa Chica, PC) including subvertical rhizoliths and encrusted terrestrial gastropods used for radiocarbon date analysis.

4.7. Stratigraphy correlation

Three sections have been constucted in this work from northeast to southwest (Figs. 13-14): Playa Chica (PC), transition sector (TS) and Colombia area (CA). PC section is composed, from bottom to top, of about 2 m of beachrock with 81% mean carbonate content. On top of this, it was found a 50 cm of weathering horizon (C-H) palaeosol, and about 2m of accumulation horizon (B-H) palaeosol, in which abundant gastropods appeared (PAC8-9). Finally, covering the palaeosol facies a 50 cm of current sands were deposited (Fig. 13). TS section corresponds to 50 cm of beachrock and 30cm of C-H about 25 cm of B-H. Covering the palaeosol is about 30 cm of current sands. The CA section is composed of about 60 cm of beachrock, 60 cm of C-H and about 2 m of B-H, 30 cm of aeoleanites and covering all 40 cm of current sands facies. The thickest beachrock outcrop (and section) was found in PC. Meanwhile, the thickest palaeosol was found in PC, being CA the only place where aeoleanites were observed.

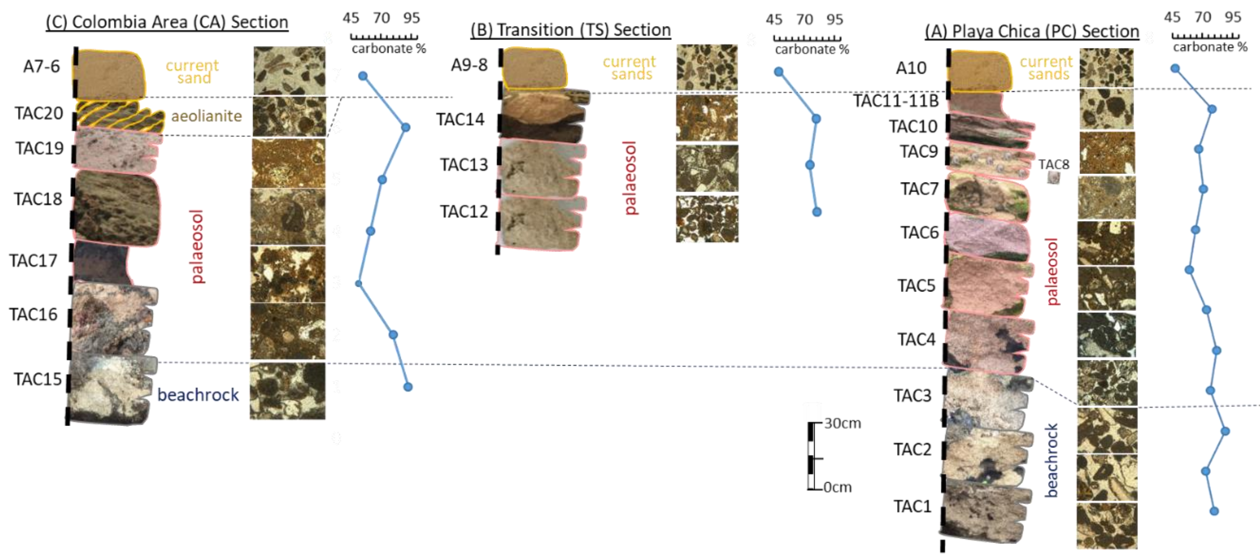

Figure 13. Stratigraphic columns for sampling sections in Las Canteras beach A) Playa Chica (PC) B) Transition (TS) and C) Colombia area (CA). At the right of the section, the petrographic microscopy image of each sample and the carbonate content curve, in percentage.

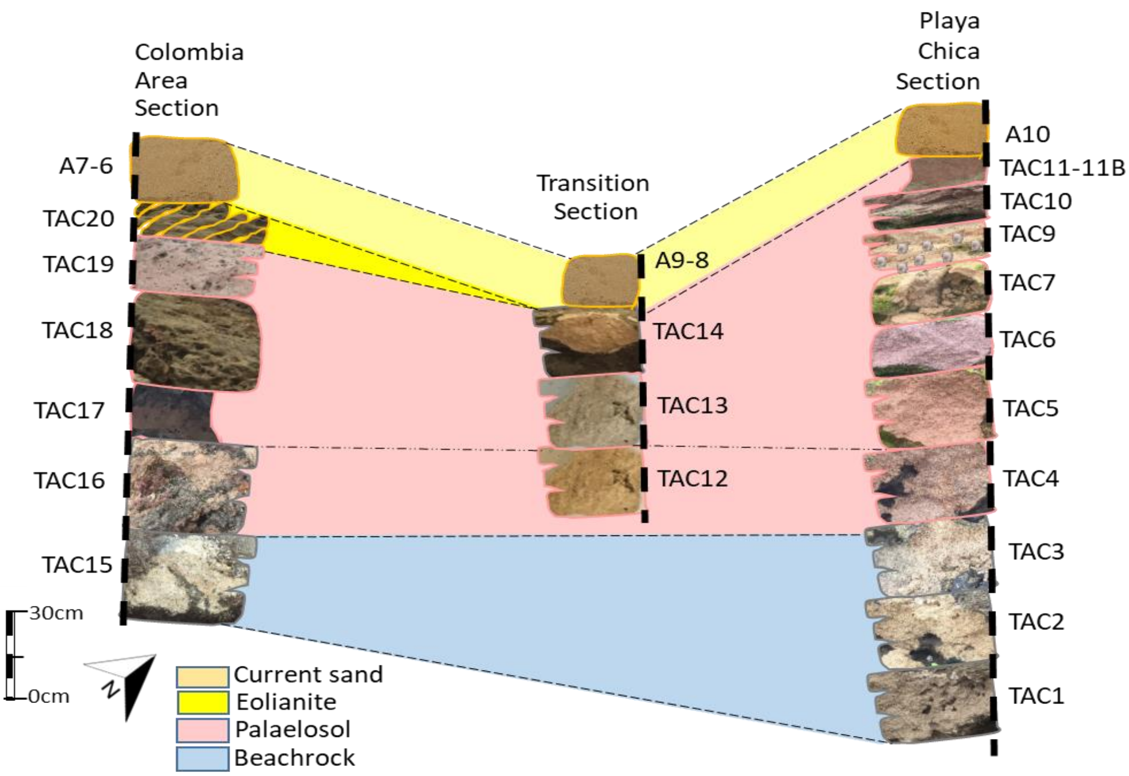

Figure 14. Stratigraphic correlation between the three studied sections in Las Canteras beach, from southwest to northeast: CA, TS and PC sections.

5. Discussion

5.1. Compiling textural, geochemical, mineralogical and datation results

Isopaque LMC in Las Canteras beachrock seem reflects meteoric waters rather than the typical (HMC) cementation of shallow marine conditions. Its presents a distinctive LMC cementation of supratidal environments (Vieira and Ros, 2007; Kelletat 2006). By other hand, LMC can precipitate in the upper intertidal part of the beachrock, where high meteoric groundwater table in the backshore exist (Tucker and Wright, 1990). Another possible scenario is a beach progradation, where beach sediment, or a pre-existent HMC beachrock could be dissolved and recrystallized, by meteoric diagenesis, under an edaphic context (Beier 1985). No remains of a HMC or dissolution features have been observed, thus, the most plausible scenario would be a primary LMC meteoric beachrock, due to a potentially abundant meteoric aquifer (intertidal scenario) or, to meteoric diagenesis related with vadose-edaphic activity (vadose scenario). Both scenarios might happened if the two LMC cementation generations are interpreted as an initial intertidal scenario (primary micritic cement) and subsequently vadose scenario (second sparitic cementation). In agreement with the asseveration of the more Mg the pore fluid content, the smaller calcite crystals will be (Mauz et al. 2015).

Las Canteras beachrock outcropping 4.5 m, thus it can be consider a thick formation, which could reflect a marked sea level fluctuation (Vieira and Ros, 2007). Besides, the optimal environment for beachrock formation is feasibly by a sea-level regression tendency or by an uplift context (Kelletat 2006), or a coastal progradation in Las Canteras beachrock formation.

Both beachrock and aeoleanites share the LMC cement occurrence (Figs. 7A-B-E-F, 10 A-B-E-F, 11B-F). LMC meteoric cementation would be favoured in the coastal dunes immersion, with an abundant meteoric groundwater (intertidal scenario). Besides, a secondary cementation of acicular rhombic aragonite in the aeoleanites (Figs. 7E-F, 10E-F, 11F), may be also formed in the marine phreatic environment, where it precipitates from agitated seawater during repeated cycles of exposure, evaporation and immersion (Desruelles et al., 2009). Higher Sr concentration observed in the aeolian aragonite (Table 5), might indicate a recent cementation (McCutcheon et al., 2017). Beachrocks characterise a rapid cementation (<5 years; Wiles et al. 2018), thus, perhaps, aragonite cementation is at present formed. Current sandy beach condition is, perhaps coetaneous with the second aragonite cement in aeoleanites facies.

Identifying petrographic evolution between facies (Fig. 8), the bioclast content decreases while the lithoclast increases from beachrock to palaeolosol. It might connected to the soil activity of the fulvic acids that dilute and redistribute, on vadose conditions, the carbonate with the subsequent formation of intraclasts and silty-clay matrix (cutans). It can be shown in Fig. 7, that the partial porous cementation in the beachrock is reduced in the palaeolosol (Fig. 7 A-B, C-D). The appearance of edaphic features together with a decrease of porosity in PC and TS could be related to a net positive balance in the edaphic accumulation in regards to dissolution process, and inversely to CA. Two palaeosol cements has been identified, a micritic mud cementation of the palaeosol matrix, possibly associated with meteoric vadose waters (Figs. 7C-D, 10C-D, 11D). Then, a secondary sparitic microcrystals generation might precipitate. Both cementations may be included in a calcretisation process (Alonso-Zarza and Wright, 2010).

The occurrence of quartz in this palaeosol reflects the existence of Saharan dust events during its formation (Menéndez et al., 2007). Quartz has been identified in the Canary islands as an exotic mineral, due to that the silica-subsaturated nature of protoliths precludes the occurrence of quartz in this volcanic rocks paragenesis (Carracedo et al., 2002). The mean quartz concentration of Gran Canaria soils is about 38% (Menéndez et al., 2007), 6% less in the mean quartz value of Las Canteras palaeosol (32%), and 7% more than in Pleistocene palaeosol (25%; Menéndez et al., 2018).

Las Canteras beachrock has been included in “La Barra” formation (Balcells et al., 1990; Pérez-Torrado and Mangas, 1992; Alonso, 1993), being part of La Terraza Baja de Las Palmas (Last Interglacial MIS5e, Meco et al., 2002). However, the mineralogical, petrographic and stratigraphic characteristics besides the distinguishing warm fauna and flora from the MIS 5e identified in marine terraces of the Eastern Canary Islands (Fuerteventura, Lanzarote and Gran Canaria; Balcells et al., 1990; Meco et al., 2002; Zazo et al., 2002) do not correspond to those founded in Las Canteras beachrock. The hypothesis is that Las Canteras beachrock would correspond to a younger period, to a Lower Holocene, because a complete absence of MIS 5e fossils, phreatic LMC cementation, sand composition similar to Las Canteras current sands, and Middle Holocene terrestrial gastropod from of the upper edaphized level. Also, it is not that unusual as there are various reported beachrock in the literature for Holocene ages in the Canary Islands and around the world (Vousdoukas et al., 2007; Mangas et al., 2008). The formation of Las Canteras beachrock had been formed before the palaeolosol developed on it, ^{14}C dated by a gastropod shell on 6.6 ka, and that before the aeoleanites (<6.6 ka) that topping the palaeolosol. The palaeosol correlate with a similar date (6.2 ka, Hansen and Criado-Hernández, 1996) from a terrestrial gastropods collected in an alluvial deposit of La Ballena Gully. This age corresponds to a climatic optimum into a high stand sea level. Therefore, the progradation of the alluvial middle Holocene fan of La Ballena gully (Hansen and Criado-Hernández, 1996), might contributed to the necessary coastal progradation in Las Canteras area for this subaerial deposits. Another aspect to take in consideration is the progressive and continuous isostatic uplift of the coast area, due to the fluvial erosion of the island (Menéndez et al., 2008). This palaeosol corresponds to the first stage of the climatic optimum, with still low stand fluctuation levels for this period.

Alonso (1993) estimated the aeoleanites age to Flandrian period (10 ka), after these coastal dunes immersion. However, accordingly to the gastropod datation, it should be Upper Holocene (<6.6 ka). Additionally, aeoleanites have been reported southern, in Maspalomas coastal dunefield (Hernández-Calvento, 2002), interpreted as well as ancient dunes but with undetermined age.

5.2. Palaeoclimatic reconstruction

This palaeoclimatic reconstruction of Las Canteras beach was constructed in four stages, starting with the sandy beach sedimentation (Stage I; Fig. 15), that will constitute the beachrock skeletal. This seaward-deepening stratified body, may have been deposited on the foreshore-intertidal environment. Then, LMC cementation in the foreshore-intertidal position might formed the beachrock, thanks to a high and abundant meteoric groundwater table in the backshore (intertidal scenario). It could be attributed to about 13ka or 10ka rising sea levels, after the cooling Younger Dryas (Fig. 16). Las Canteras beachrock could also be built during a coastal progradation (Stage II), where meteoric diagenesis linked with edaphic activity had had produced the LMC, welding the foreshore-intertidal sand body (vadose scenario). In this situation, a well-developed soil would established on the beachrock, producing both weathering (C-H) and accumulation (B-H) horizons. Rhizoliths and terrestrial gastropods were found in B-H, being the latter ^{14}C dated on 6.6 ka. This age might correspond with the second beachrock cementation, in the vadose scenario. Second spar cement generation of Las Canteras beachrock would progress at the same time than the palaeolosol, during a 6.6 ka rising sea level but, otherwise necessary, coastal progradation for beachrock edaphization. Contemporary to this temperature improvement, Corralejo and La Monja beachrocks, in Fuerteventura, were forming (Meco et al., 2018).

Following the geological sequence, the next preserved facies corresponds to the aeoleanites, vestige of an ancient coastal dunefield, developed probably on a sea transgression (Stage III), the most favourable context to form those coastal dunes (Pye and Bowman, 1984). Subsequently, aeoleanites formation by LMC meteoric cementation would be favoured during the coastal dunes immersion, due to the progressing transgression, with an abundant meteoric groundwater (intertidal scenario). These sand dunes and its cementation might correspond to the 2-3 ka rising sea level period (Fig. 15), contemporary with La Jaqueta and El Matorral beachrocks formation in Fuerteventura (Meco et al., 2018). Stage IV may represent the current sandy beach condition, perhaps coetaneous with the second aragonite cement generation in the aeoleanites facies (intertidal scenario). In this case, the abundant meteoric groundwater might proceed from the urban groundwater.

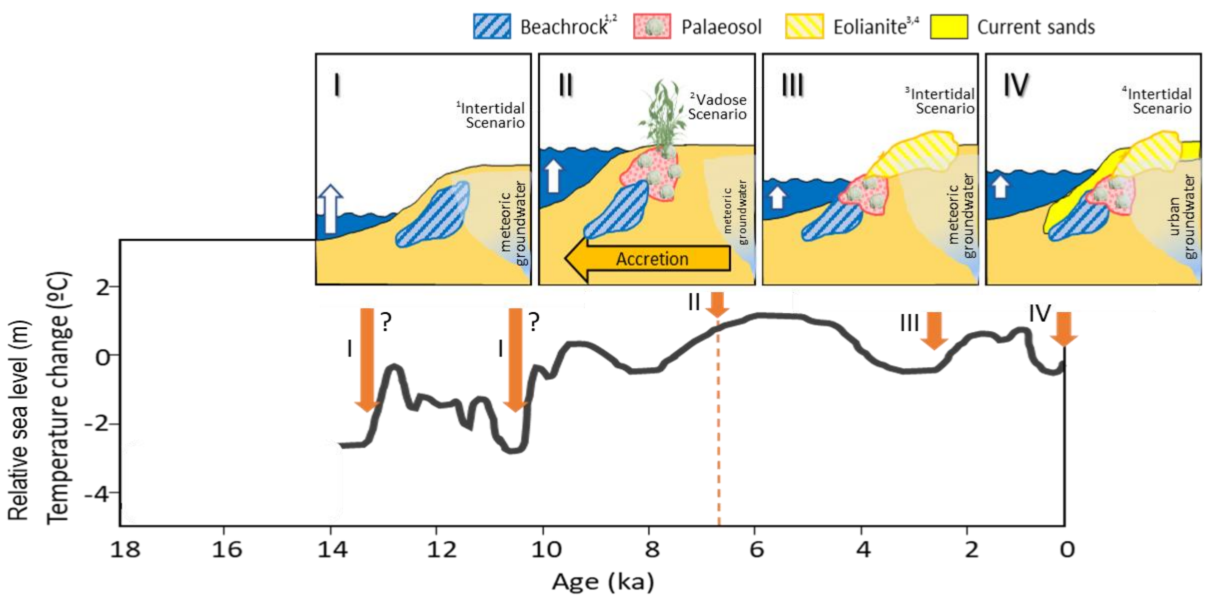

Figure 15. The four stages (I-IV) proposed for Las Canteras beach palaeoenvironments, indicating the proposed position through Upper Pleistocene-Quaternary. Orange pointed line indicating around 6.6 ka (^{14}C dated terrestrial gastropods from the palaeosol). Temperature change and relative sea

level curve assembled from Barusseau et al., 1989, accordingly Meco et al. 2018, the best fitting for Canary Islands during the last 6.5ky; and from 6.5 to 13ky based on reconstructed air temperatures from the Greenland GISP2 Ice core, Platt et al., (2017).

6. **Conclusions**

The present work is a multidisciplinary study of the Las Canteras beach outcrops that permit to gather essential information to understand the palaeoenvironmental changes of this coastal area. The main results obtained in this research are:

i) Four facies were identified. Their chronological order is (1) Upper Pleistocene-Lower Holocene Beachrock facies, with a first LMC micritic cementation (>6.6 ka). (2) Middle Holocene Palaeosol facies, accompanying a second LMC spar beachrock cementation ^{14}C dated (~6.6 ka). (3) Upper Holocene Aeoleanites facies with a first LMC micritic cementation (<6.6 ka), and (4) Current sands facies, accompanying a second aragonite cementation in aeoleanites.

ii) Petrographic study showed that the carbonate fraction is comparable in all facies and composed of bioclasts (mostly algae mesh, 17%, and mollusc, 7%). Lithoclasts are predominantly constituted by sedimentary intraclasts (8%) and felsic rocks (6%). The carbonate cement around the sand grains are crystals of micrite and sparite. The beachrock and aeoleanites petrographic configuration is similar (abundance of bioclasts, Lithoclasts and cement).

iii) LMC with Sr, Na, Fe and Mn traces appear as the major cement in beachrock, palaeosol and aeoleanites, which might be precipitate in both intertidal and vadose scenarios. Also, the aeoleanites contains a second generation of dispersing aragonite crystals, rich in Sr, probably formed recently.

iv) The presence of quartz in the soil samples (32%) evidence the Saharan dust accumulation in this environment during middle Holocene period, in minor amount that nowadays (38%) but greater than in the Pleistocene (25%).

v) Four stages have been defined in the palaeoclimatic reconstruction of Las Canteras beach (Fig. 16). Stage I: deposition of the foreshore-intertidal sand body, LMC micritic cementation in an intertidal scenario due to an abundant meteoric groundwater in the backshore. Stage II: coastal progradation with meteoric diagenesis due to beachrock edaphization producing LMC sparite (vadose scenario). Stage III: coastal dunefield development, probably during transgression and, subsequently immersion and aeoleanites formation, by LMC cementation, within an abundant meteoric groundwater (intertidal scenario). Stage IV: represents the current sandy beach, possibly coetaneous with the second aragonite cement generation in the aeoleanites (intertidal scenario), with abundant urban groundwater.

Acknowledgments

This work was supported by the CSO2016-79673-R and CSO2010-18150 research projects, both funded by the Government of Spain, and by The Municipality of Telde (Gran Canaria).

CONFILT OF INTEREST

No conflict of interest was reported by the authors.

References

Alonso, I., 1993. Procesos sedimentarios en la playa de Las Canteras (Gran Canaria). Ph D Disertation. Universidad de Las Palmas de Gran Canaria.

Alonso, I., 1994. Spatial beach morphodynamics: an example from Canary Islands. Littoral 94, 159–177.

Alonso, I., 2005. Costa Norte: Playa De Las Canteras. In: Tendencias actuales en Geomorfología Litoral. L. Hernández-Calvento, I. Alonso, J. Mangas, A. Yanes (Eds.). Universidad de Las Palmas de Gran Canaria. pp. 219–238.

Alonso, I., Vilas, F., 1994. The influence of boundary conditions on beach zonation. Coastal Dynamics 94, 417–431.

Alonso, I., Vilas, F., 1996. Variabilidad sedimentaria en la playa de Las Canteras (Gran Canaria). Geogaceta 20, 428–430.

Alonso-Zarza, A.M., Wright, V.P., 2010. Calcretes. In: Alonso-Zarza, A.M., Tanner, L.H. (eds.), Carbonates in Continental Settings: Facies, Environments, and Processes. Developments in Sedimentology Vol. 61. Elsevier, Amsterdam, pp. 225-268.

Balcells, R., Barrera-Morate, J. L., Ruiz, M.T., 1990. Mapa geomorfológico de la hoja 1101-I-II (Las Palmas de Gran Canaria). In: Mapa geológico de España 1:25.000. ITGE.

Barusseau, J.P., Descamps, C., Giresse, P., Monteillet, J., Pazdur, M., 1989. Nouvelle définition des niveaux marins le long de la côte nord-mauritanienne (Sud du Banc d'Arguin) pendant les cinq derniers millénaires. CR Acad Sci Paris. 309 (II), 1019–1024.

Beier, J.A., 1985. Diagenesis of Quaternary Bahamian beachrock: petrographic and isotopic evidence. J. Sediment. Petrol. 55(5), 755-761.

Blott, S.J., Pye, K., 2001. Technical Communication Gradistat: a Grain Size Distribution and Statistics Package for the Analysis of Unconsolidated Sediments. Earth Surface Processes and Landforms 26, 1237–1248.

Calvet, F., Cabrera, M.C., Carracedo, J.C., Mangas, J., Pérez-Torrado, F.J., Recio, C., Travé, A., 2003. Beachrocks from the island of La Palma (Canary Islands, Spain). Marine Geology 197, 75–93.

Carracedo, J.C., Day, S., Guillou, H., Rodríguez Badiola, E., Canas, J., Pérez-Torrado, F.J., 1998. Hotspot volcanism close to a passive continental margin: the Canary Islands. Geological Magazine 135(5), 591–604.

Carracedo, J.C., Pérez-Torrado, F.J., Ancochea, E., Meco, J., Hernan, F., Cubas, C.R., Casillas, R., Rodriguez, E., Ahijado, A., 2002. Cenozoic volcanism II: the Canary Islands. In: W. Gibbons, T. Moreno (Eds.). The geology of Spain, pp. 439–472.

Casalbore, D., Falese, F., Martorelli, E., Romagnoli, C., Chiocci, F.L., 2017. Submarinedepositional terraces in the Tyrrhenian Sea as a proxy for paleo-sea levelreconstruction: problems and perspective. Quat Int. 439, 169-180 http://dx.doi.org/10.1016/j.quaint.2016.02.027.

Casanova, M., 2015. Sedimentary budget on Las Canteras beach, Gran Canaria (Canary Islands, Spain). Master Disertation, Universidad de Las Palmas de Gran Canaria.

Cooper, J.A.G., Green, A.N., Wiles, E., 2017. Beachrock genesis and morphology on a paraglacial beach. Sedimentary Geology 360, 47-63. http://dx.doi.org/10.1016/j.sedgeo.2017.08.005

De Carvalho, G.S., Granja, H.M., Loureiro, E., Henriques, R., 2006. Late Pleistocene and Holocene environmental changes in the coastal zone of northwestern Portugal. Journal of Quaternary Science 21(8), 859-877.

Desruelles, S., Fouache, E., Ciner, A., Dalongeville, R., Pavlopoulos, K., Kosun, E., Coquinot, Y., Potdevin, J.L., 2009. Beachrocks and sea level changes since Middle Holocene: comparison between the insular group of Mykonos–Delos–Rhenia (Cyclades,Greece) and the southern coast of Turkey. Global and Planetary Change 66, 19–33. https://doi.org/10.1016/j.gloplacha.2008.07.009

Dickinson, W.R., 2001. Paleoshoreline record of relative Holocene sea levels on Pacific islands. Earth-Science Reviews 55, 191-234.

Falkenroth, M., Schneider, B., Hoffmann, G., 2019. Beachrock as sea-level indicator – a case study at the coastline of Oman (Indian Ocean). Quaternary Science Reviews 206, 81-98.

Ferrer-Valero, N., Hernández-Calvento, L., Hernández-Cordero, A.I., 2017. Human impacts quantification on the coastal landforms of Gran Canaria Island (Canary Islands). Geomorphology 286, 58–67.

Frébourg, G., Hasler, C.-A., Le Guern, P., Davaud, E., 2008. Facies characteristics anddiversity in carbonate eolianites. Facies 54, 175-191. https://doi.org/10.1007/s10347-008-0134-8

Friedman, G.M., 2004. Holocene chronostratigraphic beachrocks and their geologic climatic significance. Geochemical Society Special Publications 9, 125–142.

Fuster, J.M., Hernandez-Pacheco, A., Muñoz, M., Rodriguez Badiola, E., Garcia Cacho, L., 1968. Geology and volcanology of the Canary Islands, Gran Canaria. Instituto Lucas Mallada. Madrid.

Hansen, A., Criado-Hernández, C., 1996. El cono aluvial Holoceno del Barranco de La Ballena (Las Palmas de Gran Canaria). IV Reunión de Geomorfología 10, 261–270.

Haredy, R.A, Ghandour, I.M., Erginal, A.E., Bozcu, M., 2019. Beachrock Cementation Patterns Along the Gulf of Aqaba Coast, Saudi Arabia. Arabian Journal for Science and Engineering 44,479-487. https://doi.org/10.1007 /sl 3369-018-3624-1

Hernández-Calvento, L., 2002. Análisis de la evolución del sistema de dunas de Maspalomas, Gran Canaria, Islas Canarias (1960-2000). Ph D Thesis, Universidad de Las Palmas de Gran Canaria.

Hernández-Calvento, L., Mangas, J., 2004. Caracterización de los materiales sedimentarios aflorantes en el sistema de dunas de Maspalomas (Gran Canaria, Islas Canarias). In: R. Blanco-Chao, J. López Bedoya, A. Pérez-Alberti (Eds.). Procesos geomorfológicos y evolución costera: actas de la II Reunión de Geomorfología Litoral. pp. 67–81

Hulseman, J., 1966. An inventory of marine carbonate materials. Journal of Sedimentary Petrology ASCE 36 (2), 622– 625.

Jiang, T., Liu, X., Yu, T., Hu, Y., 2019. OSL dating of late Holocene coastal sediments and its implication for sea-level eustacy in Hainan Island, Southern China. Quaternary International 468, 24-32. https://doi.org/10.1016/j.quaint.2017.11.039

Kelletat, D., 2006. Beachrock as sea-level indicator? Remarks from a geomorphological point of view. J Coast Res. 22 (6), 1555–1564. : http://dx.doi.org/10.2112/04-0328

Kneale, D., Viles, H.A., 2000. Beach cementation: incipient CaCO3-cemented beachrock development in the upper intertidal zone, North Uist, Scotland. Sedimentary Geology 132, 165-170.

Mangas, J., Cabrera, L.L., Menéndez, I., Alonso, I., 2008. Beachrock, biolitita y sedimentos arenosos costeros en la playa de Famara (NE de Lanzarote). Geotemas 10, 559–562.

Mangas, J., Menendez, I., Ortiz, J.E., Torres, T., 2008. Eolianitas costeras del Pleistoceno superior en el “Sitio de Interés Científico de Tufia” (Gran Canaria): sedimentología, petrografía y aminocronología. Geotemas 1405–1408.

Martínez-Martínez, J., Espejo, A., Bilbao, A., Cabrera, R., Álvarez-Espejo, R., Alonso, I., del Rosario Cabrera, M.D., 1990. Analysis of sedimentary processes on the Las Canteras beach (Las Palmas, Spain) for its planning and management. Engineering Geology 29(4), 377–386.

Mauz, B., Vacchi, M., Green, A., Hoffmann, G., Cooper, A., 2015. Beachrock: a tool for reconstructing relative sea level in the far-field. Mar Geol. 362, 1–16. http://dx.doi.org/10.1016/j.margeo.2015.01.009

McCutcheon, J., Nothdurft, L.D., Webb, G.E., Shuster, J., Nothdurft, L., Paterson, D., Southam, G., 2017. Building biogenic beachrock: visualizing microbially-mediated carbonate cement precipitation using XFM and a strontium tracer. Chem Geol. 465, 21–34

Meco, J., Guillou, H., Carracedo, J.C., Lomoschitz, A., Ramos, A.J., Rodríguez-Yánez, J.J., 2002. The maximum warmings of the Pleistocene world climate recorded in the Canary Islands. Palaeogeography Palaeoclimatology Palaeoecology 185(1), 197–210.

Meco, J., Muhs, D.R., Fontugne, M., Ramos, A.J.G., Lomoschitz, A., Patterson, D., 2011. Late Pliocene and Quaternary Eurasian locust infestations in the Canary Archipelago. Lethaia 44(4), 440–454.

Meco, J., Lomoschitz, A., Rodríguez, Á., Ramos, A. J. G., Betancort, J.F., Coca, J., 2018. Mid and Late Holocene sea level variations in the Canary Islands. Palaeogeography Palaeoclimatology Palaeoecology 507, 214–225. https://doi.org/10.1016/j.palaeo.2018.07.020

Menéndez, I., Díaz-Hernández, J.L., Mangas, J., Alonso, I., Sánchez-Soto, P.J., 2007. Airborne dust accumulation and soil development in the North-East sector of Gran Canaria (Canary Islands, Spain). Journal of Arid Environments 71(1), 57–81. http://dx.doi.org/10.1016/j.jaridenv.2007.03.011

Menéndez, I., Silva, P.G., Martín-Betancor, M., Pérez-Torrado, F.J., Guillou, H., Scaillet, S. 2008. Fluvial dissection, isostatic uplift, and geomorphological evolution of volcanic islands (Gran Canaria, Canary Islands, Spain). Geomorphology 102(1), 189–203. http://dx.doi.org/10.1016/j.geomorph.2007.06.022

Menéndez, I., Mangas, J., Tauler, E., Barrón, V., Torrent, J., Betancort, J. F., Santana, A., Recio, J.M., Quevedo-González, L.A., Alonso, I., Méndez-Ramos, J., 2018. Aeolian influx and related environmental conditions on Gran Canaria during the early Pleistocene. Quaternary Research 1–16. https://doi.org/10.1017/qua.2018.64

Menéndez, I., Campeny, M., Quevedo-González, L., Mangas, J., Llovet, X., Tauler, E., Barrón, V., Torrent, J., Méndez-Ramos, J., 2019. Distribution of REE-bearing minerals in felsic magmatic rocks and paleosols from Gran Canaria, Spain: Intraplate oceanic islands as a new example of potential, non-conventional sources of rare-earth elements, Journal of Geochemical Exploration https://doi.org/10.1016/j.gexplo.2019.06.007

Murray-Wallace, C.V., 2002. Pleistocene coastal stratigraphy, sea-level highstands and neotectonism of the southern Australian passive continental margin - A review. Journal of Quaternary Science 17(5–6), 469–489.

Ortiz, J.E., Torres, T., Yanes, Y., Castillo, C., De la Nuez, J., Ibáñez, M., Alonso, M.R., 2006. Climatic cycles inferred from the aminostratigraphy and aminochronology of Quaternary dunes and palaeosols from the eastern islands of the Canary Archipelago. Journal of Quaternary Science 21(3), 287–306.

Pérez-Torrado, F.J., Alonso, I., 1992. Estudio sedimentológico de la playa de Las Canteras (Gran Canaria). Datos preliminares. III Congreso Geológico de España 2, 131–135.

Pérez-Torrado, F.J., Mangas, J., 1992. Origen y evolución geológica de la barra de las Canteras (Las Palmas de Gran Canaria). Vector Plus 4–13.

Pérez-Torrado, F.J., Calvet, F., Cabrera, M.C., Mangas, J., 2000. Estudio de los depósitos litorales de la playa de Las Canteras, Las Palmas de Gran Canaria. Taller y Tertulia de Oceanografía, 2.

Platt, D.E., Haber, M., Dagher-Kharrat, M.B., Douaihy, B., Khazen, G., Ashrafian Bonab, M., Salloum, A., Mouzaya, F., Luiselli, D., Tyler-Smith, C., Colin Renfrew, C., Matisoo-Smith, E., Zalloua, P.A., 2017. Mapping post-glacial expansions: the peopling of Southwest Asia. Sci Rep. 7, 40338. http://dx.doi:10.1038/srep40338

Pye, K. Bowman, G.M., 1984. The Holocene marine transgression as a forcing function in episodic dune activity on the eastern Australian coast. In: THOM, B.G. (Ed.), Coastal Geomorphology in Australia. Sydney. Academic Press, pp. 179-192.

Rodriguez-Gonzalez, A., Fernandez-Turiel, J.L., Perez-Torrado, F.J., Hansen, A.R., Aulinas, M., Carracedo, J.C., Gimeno, D., Guillou, H., Paris, R., Paterne, M.,

2009. The Holocene volcanic history of Gran Canaria island: implications for volcanic hazards. Journal of Quaternary Science 24, 697–709.

Santana-Cordero, A.M., Bürgi, M., Hersperger, A.M., Hernández-Calvento, L., Monteiro-Quintana, M.L., 2017. A century of change in coastal sedimentary landscapes in the Canary Islands (Spain): change, processes, and driving forces. Land Use Policy 68, 107–116. http://dx.doi.org/10.1016/j.landusepol.2017.07.028

Schmincke, H.U., Freundt, A., 1990. Gran Canaria: Geological Field Guide. Pluto Press.

Schmincke, H.U., Sumita, M., 1998. Volcanic evolution of Gran Canaria reconstructed from apron sediments: synthesis of vicap project drilling. Proceedings of the Ocean Drilling Program, Scientific Results 157(23), 443–469.

Schneider, J.L., Pérez-Torrado, F.J., Gimeno Torrente, D., Wassmer, P., Cabrera Santana, M.C., Carracedo, J.C., 2004. Sedimentary signatures of the entrance of coarse-grained volcaniclastic flows into the sea: The example of the breccia units of the Las Palmas Detritic Formation (Mio - Pliocene, Gran Canaria, Eastern Atlantic, Spain). Journal of Volcanology and Geothermal Research 138(3–4), 295–323.

Schmincke, H.U., Sumita, M., 2010. Geological evolution of the Canary Islands: a young volcanic archipelago adjacent to the old African Continent. Görres, Koblenz (Ed.) 200 pp.

Sperazza, M., Moore, J.N., Hendrix, M.S., 2004. High-Resolution Particle Size Analysis of Naturally Occurring Very Fine-Grained Sediment through Laser Diffractometry. Journal of Sedimentary Research 74(5), 736–743.

Spurgeon, D., Davis, R.A.J., Shinnu, E.A., 2003. Formation of 'Beach Rock' at Siesta Key, Florida and its influence on barrier island development. Marine Geology 200, 19–29. http://dx.doi:10.1016/S0025-3227(03)00162-2

Strasser, A., Davaud, E., 1986. Formation of Holocene limestone sequences by progradation, cementation, and erosion: two examples from the Bahamas. J Sediment Petrol. 56, 422–428.

Stuiver, M., Braziunas, T.F., 1993. Modeling atmospheric 14C influences and ^{14}C ages of marine samples to 10 000 BC. Radiocarbon 35(1), 137–189.

Talma, A.S., Voguel, J.C., 1993. A simplified approach to calibrating ^{14}C dates. Radiocarbon 35(2), 317–322.

Tucker, M.E., Wright, V.P., 1990. Carbonate Sedimentology. Blackwell Scientific, Oxford. 482 pp.

Vieira, M.M., De Ros, L.F., 2007. Cementation patterns and genetic implications of Holocene beachrocks from northeastern Brazil. Sediment Geol. 192 (3–4), 207–230. http://dx.doi.org/10.1016/j.sedgeo.2006.04.011

Vousdoukas, M.I., Velegrakis, A.F., Plomaritis, T.A., 2007. Beachrock occurrence, characteristics, formation mechanisms and impacts. Earth-Science Reviews 85(1–2), 23–46. http://dx.doi.org/10.1016/j.earscirev.2007.07.002

Walker, G. 1990. Geology and Volcanology of the Hawaiian Islands. Pacific Science, 44(4), 315–347.

Wiles, E., Green, A.N., Cooper, J.A.G., 2018. Rapid beachrock cementation on a South African beach: Linking morphodynamics and cement style. Sedimentary geology 378, 13-18. https://doi.org/10.1016/j.sedgeo.2018.10.004

Yao, Z., Shi, X., Li, X., Liu, Y., Liu, J., Qiao, S., Bai, Y., Wang, X., Zhu, A., Wang, X., 2017. Sedimentary environment and paleo-tidal evolution of the eastern Bohai Sea, China since the last glaciation. Quat Int. 440, 129–138. http://dx.doi.org/10.1016/j.quaint.2016.04.010

Zazo, C., Goy, J.L., Hillaire-Marcel, C., Gillot, P.Y., Soler, V., González, J.Á., Dabrio, C.J., Ghaleb, B., 2002. Raised marine sequences of Lanzarote and Fuerteventura revisited - A reappraisal of relative sea-level changes and vertical movements in the eastern Canary Islands during the Quaternary. Quaternary Science Reviews 21(18–19), 2019–2046.